Crystal structure of PRY-SPRY domain of human TRIM72.

DATASET · AUGUST 2013

CITATIONS
5

READS
91

7 AUTHORS, INCLUDING:

Byung-Cheon Jeong
University of Texas Southwestern Medical Ce…
17 PUBLICATIONS **120** CITATIONS
SEE PROFILE

Chang Seok Lee
Baylor College of Medicine
31 PUBLICATIONS **680** CITATIONS
SEE PROFILE

Young-Gyu Ko
Korea University
113 PUBLICATIONS **3,406** CITATIONS
SEE PROFILE

Hyun Kyu Song
Korea University
110 PUBLICATIONS **3,100** CITATIONS
SEE PROFILE

PROTEINS
STRUCTURE ■ FUNCTION ■ BIOINFORMATICS

STRUCTURE NOTE

Crystal structure of PRY-SPRY domain of human TRIM72

Eun Young Park[†], Oh-Bong Kwon[†§], Byung-Cheon Jeong, Jae-Sung Yi, Chang Seok Lee, Young-Gyu Ko,[*] and Hyun Kyu Song[*]

School of Life Sciences and Biotechnology, Korea University, Seoul 136-701, Korea

Key words: B30.2; gustavus; spry; TRIM21; tripartite motif.

INTRODUCTION

Tripartite motif-containing (TRIM) family proteins consist of multimodular domains including a relatively conserved N-terminal RBCC domain consisting of a RING finger for E3 ubiquitin ligase activity, a zinc-bound B-box for protein–protein interaction, one or two coiled-coil domains for oligomerization, and a variable C-terminal domain. In some cases, however, TRIM proteins have a PRY-SPRY domain (PRY segment followed SPRY domain identified in a *Dictyostelium discoidueum* kinase splA and mammalian Ca^{2+}-release channels ryanodine receptors) at their C-terminus, which has been identified as a targeting module.[1,2] More than 70 members of this family have been identified and characterized, and show a very similar domain architecture; however, their cellular functions are extremely diverse, and include roles in cell proliferation, differentiation, development, oncogenesis, apoptosis, and retroviral replication.[1,2] The E3 ligase activity of several TRIM proteins has been previously demonstrated, as they usually harbor a RING domain at the N-terminal region. Each TRIM protein interacts with distinct targets, which are critical in the aforementioned cellular processes.[3–8] Therefore, relatively newly and incompletely characterized C-terminal domains, including the PRY-SPRY domain, are believed to be a central mediator for selective interaction with their partners.

Well-studied members of the TRIM family include the following: TRIM1, TRIM5α, TRIM19, and TRIM22, which target retroviruses and prevent their replication inside cells[3,6]; TRIM18/MID1 and TRIM20/pyrin, which are linked to Opitz G/BBB syndrome and familial Mediterranean fever, respectively[2,9]; TRIM21/Ro52, which is a major autoantigen in autoimmune diseases such as rheumatoid arthritis, systemic lupus erythematosus, and Sjörgen's syndrome[10,11]; and TRIM63/Murf1, TRIM55/Murf2, TRIM41, and TRIM32, which function in muscle cells.[1,12] Recently, another TRIM family protein, TRIM72/MG53 has been shown to be expressed specifically in skeletal muscle and heart, and also been demonstrated to perform a critical function in membrane repair following acute muscle injury.[13–15] Human TRIM72 consists of 477 amino acid residues with the standard domain organization of the TRIM family [Fig. 1(A)]. By way of contrast with the RBCC domain, which is predictive of its molecular function, very little is currently known regarding the PRY-SPRY domain, or how it has evolved to mediate diverse functions in each TRIM protein.

Thus far, two structures of the SPRY domain have been determined in the complex state; however, their interac-

Abbreviations: PRYSPRY21, PRY-SPRY domain of TRIM21; PRYSPRY72, PRY-SPRY domain of TRIM72; RBCC, Ring-Bbox-Coiled Coil; TRIM, tripartite motif.

[†]Eun Young Park and Oh-Bong Kwon contributed equally to this work.
[§]Deceased

Grant sponsor: Molecular and Cellular Biodiscovery Research Program, National Research Foundation; Grant number: M10648230002-08N4823-00210; Grant sponsor: Basic Science Research Program, National Research Foundation; Grant number: NRF-2009-0083778; Grant sponsor: 21C Frontier Functional Proteomics Project; Grant number: FPR08B2-270; Grant sponsor: KIST intramural.
*Correspondence to: Hyun Kyu Song or Young-Gyu Ko, School of Life Sciences and Biotechnology, Korea University, Anam-dong, Seongbuk-gu, Seoul 136-701, Korea. E-mail: hksong@korea.ac.kr or ygko@korea.ac.kr
Received 8 October 2009; Revised 20 October 2009; Accepted 20 October 2009
Published online 30 October 2009 in Wiley InterScience (www.interscience.wiley.com). DOI: 10.1002/prot.22647

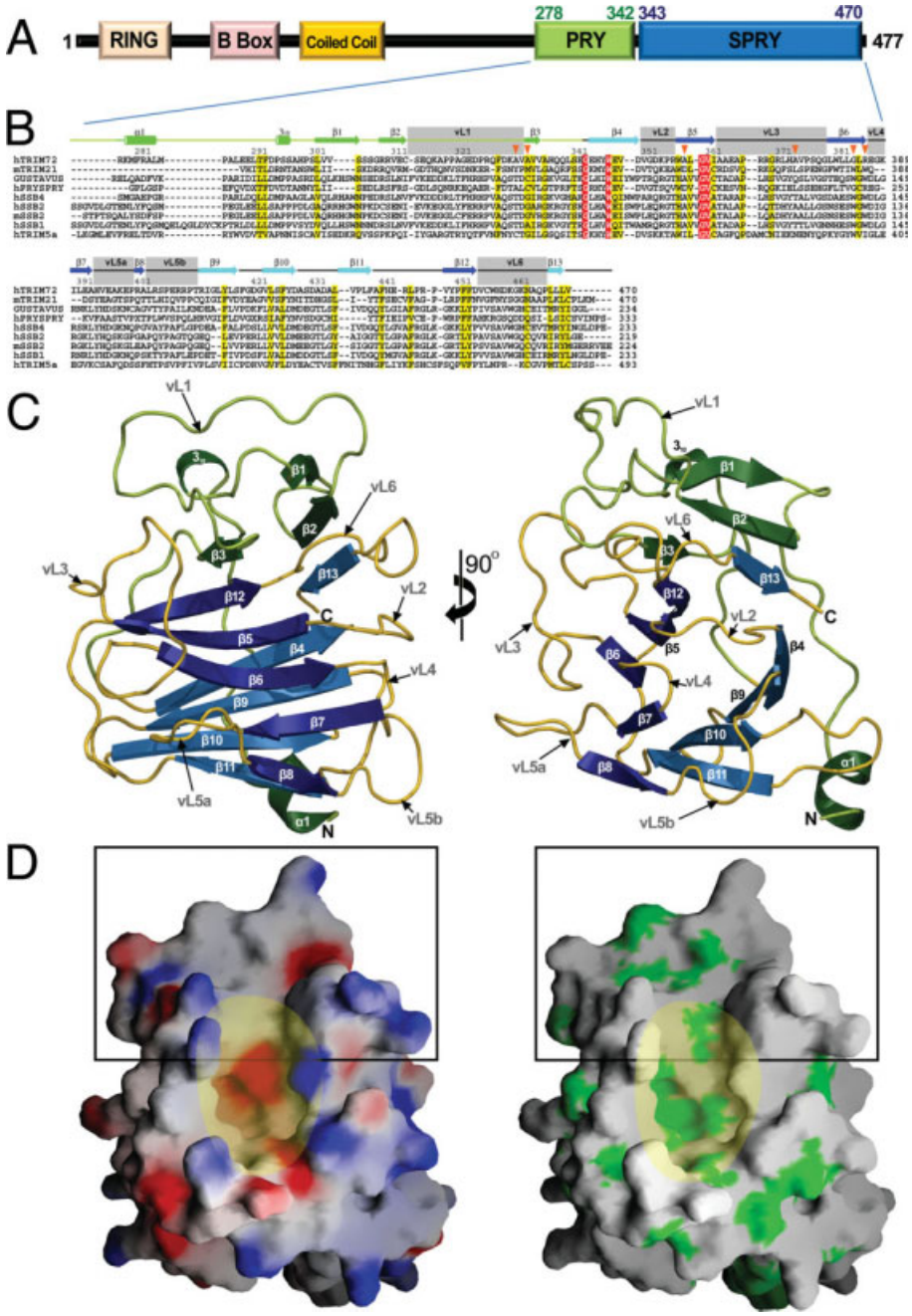

Figure 1

Overall structure of PRY-SPRY domain of TRIM72 (**A**) Domain architecture of the TRIM72 protein. As noted in the main text, the C-terminal PRY and SPRY domains are not structurally independent. (**B**) Sequence alignment among SPRY domain from human TRIM72 (hTRIM72), mouse TRIM21 (mTRIM21), *Drosophila* GUSTAVUS (GUSTAVUS), several SPRY domain containing SOCS box proteins (SSBs), and human TRIM5α (hTRIM5a). The secondary structural elements at the tops of the blocks correspond to those of TRIM72. Strictly conserved residues marked with red and yellow boxes indicate conservatively substituted residues. The residues forming a pocket for protein–protein interactions are marked with filled orange down-arrows. (**C**) Ribbon diagram showing the overall structure of PRYSPRY72 and on the right is a 90° rotation along the vertical axis as indicated. With the exception of the N-terminal PRY domains colored in green, β-sheets and connecting loops of SPRY domain are colored, blue, and yellow, respectively. The secondary structural elements are sequentially labeled and the notable variable loops are labeled in accordance with standard nomenclature. The N- and C-termini of PRYSPRY72 are also labeled. (**D**) Surface properties of PRYSPRY72. Left, electrostatic potential surface of PRYSPRY72 can be viewed in the left panel (C). Positive and negative electrostatic potentials are colored blue and red, respectively. VASA peptide binding region and prominent pocket are indicated as a black rectangle and transparent yellow oval, respectively.

Table I
Data Collection, Phasing, and Refinement Statistics

		MAD		
	Native	Peak	Edge	Remote
Data collection				
Space group	C2		C2	
Cell dimension				
a, b, c (Å)	153.75, 35.94, 33.20		151.96, 35.73, 33.18	
α, β, γ (°)	90.0, 99.87, 90.0		90.0, 98.54, 90.0	
X-ray sources[a]	PF NW12		PAL 4A	
Wavelength (Å)	1.00000	0.97951	0.97967	0.9600
Resolution (Å)[b]	1.50 (1.53–1.50)	2.20 (2.28–2.20)	2.20 (2.28–2.20)	2.20 (2.28–2.20)
R_{merge} (%)[c]	5.8 (17.0)	6.5 (22.0)	5.9 (21.2)	8.6 (31.3)
Total reflections	78,009	35,951	35,845	29,165
Unique reflections	26,011	9062	9086	8256
Completeness (%)	99.9 (99.1)	98.8 (92.0)	98.9 (91.6)	91.3 (59.2)
FOM[d]			0.34/0.64 (SOLVE/RESOLVE)	
Refinement				
Resolution range (Å)	50.0–1.5			
Reflections used	26,011			
R_{work}/R_{free} (%)[e]	21.9/23.7			
Number of atoms				
Proteins	1526			
Water	161			
R.m.s deviations				
Bond length (Å)	0.005			
Bond angles (°)	1.31			
Ramachandran outlier	0.6% (1)			
PDB ID	3KB5			

[a]PF, photon factory, Japan; PAL, Pohang Accelerator Laboratory, Korea
[b]Values in parentheses are for reflections in the highest resolution bin.
[c]$R_{merge} = \sum_h\sum_i|I(h,i) - \langle I(h)\rangle|/\sum_h\sum_i I(h,i)$, where $I(h,i)$ is the intensity of the ith measurement of h and $\langle I(h)\rangle$ is the corresponding average value for all i measurements.
[d]Figure of merit $= |\sum P(\alpha)e^{i\alpha}/\sum P(\alpha)|$, where $P(\alpha)$ is the phase probability distribution and α is the phase.
[e]R_{work} and $R_{free} = \sum||F_O| - |F_C||/\sum|F_O|$ for the working set and test set (10%) of reflections.

tion surfaces with binding partners differ markedly.[16–18] Herein, we have determined the crystal structure of the PRY-SPRY domain of human TRIM72 (PRYSPRY72) at 1.5 Å, which is the highest resolution achieved among this family of proteins thus far. The structure shares similarity with several other B30.2/SPRY domains of murine SSB-2, human *19q13.4.1* gene product, *Drosophila* SSB (GUSTAVUS), and TRIM 21.[16,17,19–22] As the B30.2/SPRY domain is believed to function as a protein–protein interaction module, this domain in TRIM72 may also be involved in such interactions. Although the binding partner of this protein has yet to be identified, the key determinants for protein–protein interaction can be proposed using this structure.

MATERIALS AND METHODS

Sample preparation

The full-length human *trim72* gene was obtained from human muscle cDNA using polymerase chain reaction (PCR). The PRY-SPRY domain of the human *trim72* gene was also cloned using the standard PCR technique. It was flanked by the BamHI and EcoRI restriction enzyme sites, and the fragments were ligated into a modified pET-GST expression vector (Novagen). The integrity of the resultant plasmids was confirmed via DNA sequencing and the plasmids were then transformed into C41(DE3) cells.[23] Protein expression was induced via the addition of 1 m*M* IPTG at OD (600 nm) = 0.8. After 20 h of induction at 18°C, the cells were harvested by centrifugation and kept frozen at –80°C until further use. The cell pellet was resuspended in ice-cold 1× PBS (phosphate buffered saline) in the presence of 1 m*M* phenylmethylsulphonyl fluoride and subsequently disrupted by ultrasonication. The proteins were applied to a glutathione affinity column as the first step. Eluents from the column were analyzed via SDS-PAGE and visualized with Coomassie blue stain. The fractions containing PRYSPRY72 were pooled and tobacco etch virus protease was added (20 μg per mg fusion protein). The GST-removed target protein was purified further by anion exchange chromatography (Mono Q 16/10 HR, GE Healthcare) and subsequently by gel filtration chromatography (Superose 12 10/30 HR, GE Healthcare). Selenomethionyl-PRYSPRY72 was expressed with B834(DE3) cells and purified as a wild-type protein.

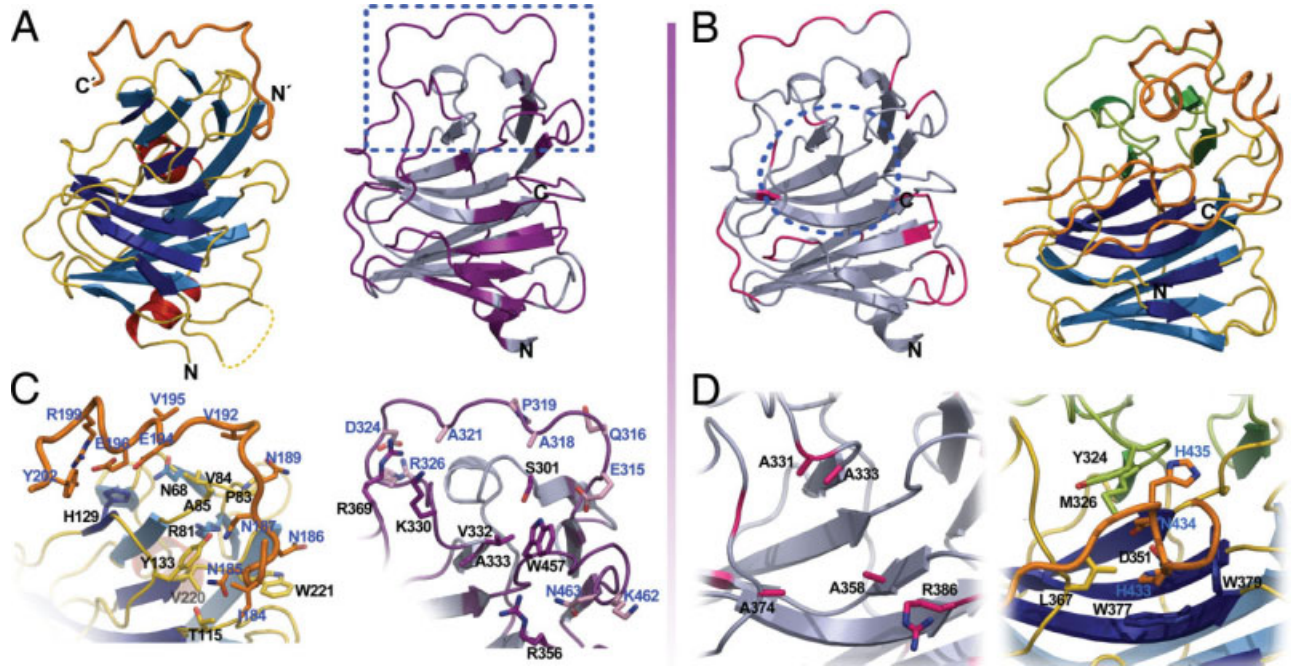

Figure 2

Structural comparisons (**A**) Structural comparisons [GUSTAVUS (left) versus PRYSPRY72 (right)]. This view is the same as in Figure 1(C) (right). The bound VASA peptide is colored orange in GUSTAVUS (left). The regions evidencing significant structural movement (>1.5 Å displacement) and structural conservation (<1.5 Å) are colored purple and gray, respectively (right). The region corresponding to the bound VASA peptide is boxed [See details for panel (C)]. (**B**) Structural comparisons [PRYSPRY72 (left) versus PRYSPRY21 (right)]. The view is the same as (A). The prominent pocket in TRIM72 is marked and it shares the same position for binding the IgG Fc fragment (drawn as orange) in TRIM21 (right). The regions evidencing significant structural movement (>1.5 Å displacement) and structural conservation (<1.5 Å) are colored red and gray, respectively (left). (**C**) Close-up view of the protein–protein interaction site in GUSTAVUS (left) and PRYSPRY72 (right), respectively. Proteins are presented as ribbon diagrams and important residues as stick models and also labeled with blue for the VASA peptide and PRY residues, and black for the SPRY residues. (**D**) Close-up view of the protein–protein interaction site in PRYSPRY72 (left) and PRYSPRY21 (right), respectively. Proteins are presented as a ribbon diagram and important residues as stick model and also labeled as blue for IgG Fc and black for PRYSPRY residues, respectively. See details for main text.

Crystallography

The purified PRYSPRY72 was concentrated to 10.2 mg/mL in 50 m*M* Tris-HCl, pH 8.0, 100 m*M* NaCl, and 5 m*M* DTT. Crystallization was conducted using the hanging-drop vapor diffusion method at 22°C. Crystals were obtained with the reservoir solution consisting of 100 m*M* Tris-HCl pH = 8.0, 20% (w/v) polyethylene glycol 3350, and 200 m*M* potassium nitrate. Crystals grew to the maximum size of 0.5 × 0.5 × 0.2 mm^3 within 1–2 days. The native diffraction data were collected on a charge-coupled device detector at the NW12 beamline of the Photon Factory, Japan. The multiwavelength anomalous dispersion data using selenomethionine derivatives were collected on a charge-coupled device detector at the 4A beamline of the Pohang Accelerator Laboratory, Korea. All diffraction data were processed and scaled using the HKL2000 software package.[24] Statistics for data collection are described in Table I.

Two of the selenium sites in the asymmetric unit were located and the phases were improved with the SOLVE/RESOLVE program.[25] The phasing statistics are described in Table I. The experimental phases were extended to 1.5 Å resolution and automatic chain tracing was conducted with ARP/wARP.[26] The nearly complete model was built and the electron density was of sufficient quality to fit the amino acid residues in accordance with the sequence information. The protein model was refined with CNS including the bulk solvent correction.[27] Solvent molecules were added using model-phased difference Fourier maps. Statistics for the refined structure are also described in Table I. Model geometry was assessed and the secondary structure elements were assigned using the PROCHECK program.[28]

RESULTS AND DISCUSSION

Overall structure

The crystals diffracted up to 1.5 Å resolution using a Synchrotron source; this is the highest resolution among

all known structures of the SPRY domains. By way of contrast with the human PRYSPRY-domain of the *19q13.4.1* gene product,[22] PRYSPRY72 exists solely as a monomer in solution (data not shown) and one copy of PRYSPRY72 is found in the asymmetric unit. The current model begins at the first residue, Arg278, and ends with the Val470 residue. The overall structure of PRYSPRY72 shows that the PRY (Leu290-Glu342) and SPRY (Gly343-Gly477) domains are not independent, as are other PRY-SPRY structures [Fig. 1(C)]17,22 and forms a compact globular structure consisting of an α-helix, 13 β-strands, and a 3_{10}-helix from both domains [Fig. 1(C)]. The primary structural feature is two antiparallel β-sheets packed against each other, and the connecting loops exhibit a unique conformation for the function [Fig. 1(C)]. These β-sheets are twisted, forming a convex surface at one side and a concave surface including a large pocket on the other side [Fig. 1(C)], which is a conserved feature among known PRY-SPRY structures;[17,22] however, the details of the structures differ profoundly.

Structural comparison with ligand-complexed SPRY structures

PRYSPRY72 shares very limited sequence identity (only 28 and 25% sequence identity with PRYSPRY21 and GUSTAVUS, respectively; 49 and 35% sequence similarity with PRYSPRY21 and GUSTAVUS, respectively) with other known SPRY domains [Fig. 1(B)], thereby suggesting potentially unique interactions with different binding partners that, in turn, lead to a wide range of roles in cellular processes. The overall superposition among SPRY domains was determined with COOT using the SSM algorithm.[29,30] When 139 matching Cα atoms of PRYSPRY72 were superposed with equivalent GUSTAVUS atoms, the average displacement was 1.88 Å. As is shown in Figure 2(A), the substantially deviating parts (>1.5 Å) between PRYSPRY72 and GUSTAVUS spread out throughout the entire structure, and in some cases the central β-strands deviated more than the loop structures [Fig. 2(A)]. In the same calculation with 171 equivalent Cα atoms of PRYSPRY21, the average displacement was only 0.94 Å. As is shown in Figure 2(B), the substantially deviating parts (>1.5 Å) between PRYSPRY72 and PRYSPRY21 are located in the connecting loops, and the interior β-strands of the molecule are structurally conserved [Fig. 2(B)]. These results imply that the structure of PRYSPRY72 differs from those of previously investigated SPRY molecules, which might have been expected from the primary sequence differences [Fig. 1(B)].

One of the most interesting structural differences between PRYSPRY72 and GUSTAVUS is that the inserted loop (vL1) in PRYSPRY72 virtually overlaps with the VASA peptide in GUSTAVUS complex structure [Fig. 2(A)]. GUSTAVUS consists of the SPRY domain only, lacking the PRY domain, and the loop between the PRY and SPRY domain in PRYSPRY replaces the binding partner of GUSTAVUS [Fig. 2(A)]. A consensus sequence motif, D-I-N-N-N-N, is found in the par-4 protein at the N-terminal portion of the VASA peptide, and it fits into the pocket of the GUSTAVUS protein [Fig. 2(A)].[16] However, a characteristic loop (vL6 near Lys460) in PRYSPRY72 protrudes out from the molecule and fills up the pocket region in GUSTAVUS. In the case of PRYSPRY21, the preformed pocket generated by structurally conserved secondary structures and connecting loops also differs substantially (see details in next section). The characteristic loops described above are not significantly different from those of PRYSPRY21; however, current docking suggests that it induces significant overlaps with the Leu314 and Asn315 residues of the IgG Fc fragment. Many differences in the loop regions located on the protein surface, including this loop, might be responsible for the differing specificities.

Putative binding pocket

The putative binding pocket of PRYSPRY72 differs substantially from those of other known proteins, as noted above, which was expected from the sequence variations [Fig. 1(B)]. It is also obvious that the protein binding site in the TRIM family differs markedly from that of GUSTAVUS, a SPRY-only B30.2 protein. An additional structural insertion (β7-Dloop-β8 region according to the secondary structure assignment of GUSTAVUS) in GUSTAVUS has been shown to completely block the corresponding region of the putative binding pocket in PRYSPRY72, and a narrow and shallow pocket for the D-I-N-N-N-N motif in a different region is formed instead.

As previously mentioned, the structural divergence with PRYSPRY21 is not particularly significant, and indeed the IgG Fc binding pocket of PRYSPRY21 shares a very similar main-chain structure with that of PRYSPRY72 [Fig. 2(B)]. However, there exist major differences in the sequence of the putative binding pocket [Fig. 1(B)]. Intriguingly, the most common variation of PRYSPRY72 forms a potential binding cleft for a smaller side-chain. The four major determinants for IgG Fc recognition in PRYSPRY21 are Asp359, Trp385, Trp387, and Phe448, and the corresponding residues in PRYSPRY72 are Ala358, Gly384, Arg386, and Phe452. Moreover, the other residues (Tyr332, Met334, and Leu375) forming the pocket structure in PRYSPRY21 are all mutated to alanines (Ala331, Ala333, Ala374) in PRYSPRY72. With the exception of Phe452 (Phe448 in PRYSPRY21) all other residues occupy a greatly reduced space due to the above substitution. Consequently, PRYSPRY72 harbors a significantly broader and deeper pocket on the putative binding surface [Fig. 1(D)].

In summary, we present herein the as-yet highest resolution images of the PRY-SPRY structure from human

TRIM72, a key molecule involved in the membrane repair process.[13] Additionally, via our structural comparison with other known SPRY structures, we have provided a clear picture of the pocket for its binding partner, although this binding partner has yet to be definitively identified, as well as the mutating residues necessary to determine the cellular function of this important molecule.

ACKNOWLEDGMENTS

The authors thank the staff at the 4A Beamline, Pohang Light Source, Korea and the NW12 beamline, Photon Factory, Japan for their help with the data collection for this study.

REFERENCES

1. Ozato K SD, Chang TH, Morse HC. TRIM family proteins and their emerging roles in innate immunity. Nat Rev Immunol 2008;8:849–860.
2. Nisole S, Stoye JP, Saib A. TRIM family proteins: retroviral restriction and antiviral defence. Nat Rev Microbiol 2005;3:799–808.
3. Eldin P, Papon L, Oteiza A, Brocchi E, Lawson TG, Mechti N. TRIM22 E3 ubiquitin ligase activity is required to mediate antiviral activity against encephalomyocarditis virus. J Gen Virol 2009;90: 536–545.
4. Vichi A, Payne DM, Pacheco-Rodriguez G, Moss J, Vaughan M. E3 ubiquitin ligase activity of the trifunctional ARD1 (ADP-ribosylation factor domain protein 1). Proc Natl Acad Sci USA 2005; 102:1945–1950.
5. Urano T, Usui T, Takeda S, Ikeda K, Okada A, Ishida Y, Iwayanagi T, Otomo J, Ouchi Y, Inoue S. TRIM44 interacts with and stabilizes terf, a TRIM ubiquitin E3 ligase. Biochem Biophys Res Commun 2009;383:263–268.
6. Duan Z, Gao B, Xu W, Xiong S. Identification of TRIM22 as a RING finger E3 ubiquitin ligase. Biochem Biophys Res Commun 2008;374:502–506.
7. Chen D, Gould C, Garza R, Gao T, Hampton RY, Newton AC. Amplitude control of protein kinase C by RINCK, a novel E3 ubiquitin ligase. J Biol Chem 2007;282:33776–33787.
8. Meroni G, Diez-Roux G. TRIM/RBCC, a novel class of 'single protein RING finger' E3 ubiquitin ligases. Bioessays 2005;27:1147–1157.
9. Berti C, Fontanella B, Ferrentino R, Meroni G. Mig12, a novel Opitz syndrome gene product partner, is expressed in the embryonic ventral midline and co-operates with Mid1 to bundle and stabilize microtubules. BMC Cell Biol 2004;5:9.
10. Rhodes DATJ. TRIM21 is a trimeric protein that binds IgG Fc via the B30.2 domain. Mol Immunol 2007;44:2406–2414.
11. Kong HJ, Anderson DE, Lee CH, Jang MK, Tamura T, Tailor P, Cho HK, Cheong J, Xiong H, Morse HC, Ozato K. Cutting edge: autoantigen Ro52 is an interferon inducible E3 ligase that ubiquitinates IRF-8 and enhances cytokine expression in macrophages. J Immunol 2007;179:26–30.
12. Kudryashova E, Kudryashov D, Kramerova I, Spencer MJ. Trim32 is a ubiquitin ligase mutated in limb girdle muscular dystrophy type 2H that binds to skeletal muscle myosin and ubiquitinates actin. J Mol Biol 2005;354:413–424.
13. Cai CMH, Weisleder N, Matsuda N, Nishi M, Hwang M, Ko JK, Lin P, Thornton A, Zhao X, Pan Z, Komazaki S, Brotto M, Takeshima H, Ma J. MG53 nucleates assembly of cell membrane repair machinery. Nat Cell Biol 2009;11:55–64.
14. Cai CMH, Weisleder N, Pan Z, Nishi M, Komazaki S, Takeshima H, Ma J. MG53 regulates membrane budding and exocytosis in muscle cells. J Biol Chem 2009;284:3314–3322.
15. Cai CWN, Ko JK, Komazaki S, Sunada Y, Nishi M, Takeshima H, Ma J. Membrane repair defects in muscular dystrophy are linked to altered interaction between MG53, caveolin-3 and dysferlin.. J Biol Chem 2009;284:15894–15902.
16. Woo JSSH, Park SY, Oh BH. Structural basis for protein recognition by B30.2/SPRY domains. Mol Cell 2006;24:967–976.
17. James LCKA, Khan Z, Rhodes DA, Trowsdale J. Structural basis for PRYSPRY-mediated tripartite motif (TRIM) protein function. Proc Natl Acad Sci USA 2007;104:6200–6205.
18. Keeble AHKZ, Forster A, James LC. TRIM21 is an IgG receptor that is structurally, thermodynamically, and kinetically conserved. Proc Natl Acad Sci **USA** 2008;105:6045–6050.
19. Masters SLYS, Willson TA, Zhang JG, Palmer KR, Smith BJ, Babon JJ, Nicola NA, Norton RS, Nicholson SE. The SPRY domain of SSB-2 adopts a novel fold that presents conserved Par-4-binding residues. Nat Struct Mol Biol 2006;13:77–84.
20. Woo JSIJ, Min CK, Kim KJ, Cha SS, Oh BH. Structural and functional insights into the B30.2/SPRY domain. EMBO J 2006;25:1353–1363.
21. Kuang ZYS, Xu Y, Lewis RS, Low A, Masters SL, Willson TA, Kolesnik TB, Nicholson SE, Garrett TJ, Norton RS. SPRY domain-containing SOCS box protein 2: crystal structure and residues critical for protein binding. J Mol Biol 2009;386:662–674.
22. Grütter CBC, Capitani G, Mittl PR, Papin S, Tschopp J, Grütter MG. Structure of the PRYSPRY-domain: implications for autoinflammatory diseases. FEBS Lett 2006;580:99–106.
23. Miroux B, Walker JE. Over-production of proteins in *Escherichia coli*: mutant hosts that allow synthesis of some membrane proteins and globular proteins at high levels. J Mol Biol 1996; 260:289–298.
24. Minor W, Tomchick D, Otwinowski Z. Strategies for macromolecular synchrotron crystallography. Structure 2000;8:R105–110.
25. Terwilliger T. SOLVE and RESOLVE: automated structure solution, density modification and model building. J Synchrotron Radiat 2004;11:49–52.
26. Perrakis A, Morris R, Lamzin VS. Automated protein model building combined with iterative structure refinement. Nat Struct Biol 1999;6:458–463.
27. Brunger AT, Adams PD, Clore GM, Delano WL, Gros P, Grosse-Kunstleve RW, Jiang JS, Kuszewski J, Nilges M, Pannu NS, Read RJ, Rice LM, Simonson T, Warren GL. Crystallography and NMR system: a new software suite for macromolecular structure determination. Acta Crystallogr D 1998;54:905–921.
28. Laskowski R, Macarthur M, Hutchinson E, Thorton J. PROCHECK: a program to check the stereochemical quality of protein structures. J Appl Crystallogr 1993;26:283–291.
29. Emsley P, Cowtan K. Coot: model-building tools for molecular graphics. Acta Crystallogr D Biol Crystallogr 2004;60:2126–2132.
30. Krissinel E, Henrick K. Secondary-structure matching (SSM), a new tool for fast protein structure alignment in three dimensions. Acta Crystallogr D Biol Crystallogr 2004;60:2256–2268.